ELSEVIER

Journal of Organometallic Chemistry 571 (1998) 289–295

Journal of Organometallic Chemistry

Preparation and crystal structures of $[\mu\text{-}SbPh_2]_2[Mo(CO)_2(\eta^5\text{-}C_5H_5)]_2 \cdot CHCl_3$ and $SbPh[Fe(CO)_2(\eta^5\text{-}C_5H_5)]_2$

Martin N. Gibbons, D. Bryan Sowerby *

Department of Chemistry, University of Nottingham, Nottingham NG7 2RD, UK

Received 17 June 1998

Abstract

Antimony is reduced when $[SbPh_2BrO]_2$ is treated with $Na[Mo(CO)_3(\eta^5\text{-}C_5H_5)]$ to produce $[\mu\text{-}SbPh_2]_2[Mo(CO)_2(\eta^5\text{-}C_5H_5)]_2$. A structure determination shows diphenylstibido groups bridging between two $Mo(CO)_2(\eta^5\text{-}C_5H_5)$ moieties giving a central 'butterfly' shaped Sb_2Mo_2 ring. The cyclopentadiene rings are *trans* to each other and Mo–Sb and Sb–Sb separations are both short. An iron analogue could not be obtained from $[SbPh_2BrO]_2$ and $Na[Fe(CO)_2(\eta^5\text{-}C_5H_5)]$ but a mixture of $SbPh[Fe(CO)_2(\eta^5\text{-}C_5H_5)]_2$ and $SbPh_2[Fe(CO)_2(\eta^5\text{-}C_5H_5)]$ was obtained using $SbPh_2Cl$. An X-ray structure for $SbPh[Fe(CO)_2(\eta^5\text{-}C_5H_5)]_2$ shows an open stibinidine structure.

Keywords: Antimony; Cyclopentadiene; Stibinidine

1. Introduction

Low oxidation state transition metal moieties readily bond to ligands containing Group 15 elements with phosphorus and arsenic compounds being the most widely investigated. Although fewer antimony analogues are known, there are examples of coordination by tertiary stibines, e.g. $Fe(CO)_4(SbPh_3)$ [1] and bridging by either distibines, e.g. $[Cr(CO)_5]_2(\mu_2\text{-}Sb_2Ph_4)$ [2] or oxo-distibines, e.g. $[Ni(CO)_2]_2(\mu_2\text{-}SbPh_2OSbPh_2)_2$ [3]. SbR_2 and SbR fragments and even naked antimony atoms can bridge between 17-e$^-$ fragments giving products such as $SbR_2[Fe(CO)_2(\eta^5\text{-}C_5H_5)]$, where R = Me or Br, [4], $SbCl[M(CO)_n(\eta^5\text{-}C_5H_5)]_2$, where M = Mo or W, $n = 3$ and M = Fe, $n = 2$ [5], $SbMe[Fe(CO)_2(\eta^5\text{-}C_5H_5)]_2$ [6] and $Sb[Re(CO)_5]_3$ [7]. 'Open' and 'closed', i.e. containing an additional M–M bond, tautomeric forms are known for $SbR[ML_n]_2$ compounds. Antimony species, such as Sb_2 and RSb = SbR, are unknown as free entities but can be stabilised in complexes such as $[Mo(CO)_2(\eta^5\text{-}C_5H_5)]_2(\mu,\eta^2\text{-}Sb_2)$ [8] and $[SbBu^t{=}SbBu^t][Cr(CO)_5]_3$ [9]. This general area has been reviewed recently [10].

There are few compounds containing antimony in a higher oxidation state and such species may be rare in view of the reducing conditions provided by the transition metal species used. Two compounds that have been isolated are $SbMe_2Cl_2[Fe(CO)(PMe_3)(\eta^5\text{-}C_5H_5)]$ [11] and $SbRf_2[Fe(CO)_2(\eta^5\text{-}C_5H_5)]$, where Rf = $o\text{-}C_6H_4C(CF_3)_2O$– [12] and it is interesting that solutions of $(\mu\text{-}Sb_2)[Co(CO)_2PR_3]_2$, where R = Ph or *p*-tolyl, can be oxidised to $[SbO(OH)][Co(CO)_3(PR_3)]_2$, a further higher oxidation compound containing a ligand unknown as a free entity [13]. As higher oxidation state antimony fragments have been stabilised in low oxidation state transition metal complexes and in the hope of preparing further examples, we have examined reactions of $[SbPh_2BrO]_2$, which contains a stable Sb_2O_2 ring with, initially, $Na[Mo(CO)_3(\eta^5\text{-}C_5H_5)]$ and $Na[Fe(CO)_2(\eta^5\text{-}C_5H_5)]$.

* Corresponding author. Fax: +44 115 9513563.

0022-328X/98/$ - see front matter
PII S0022-328X(98)00898-5

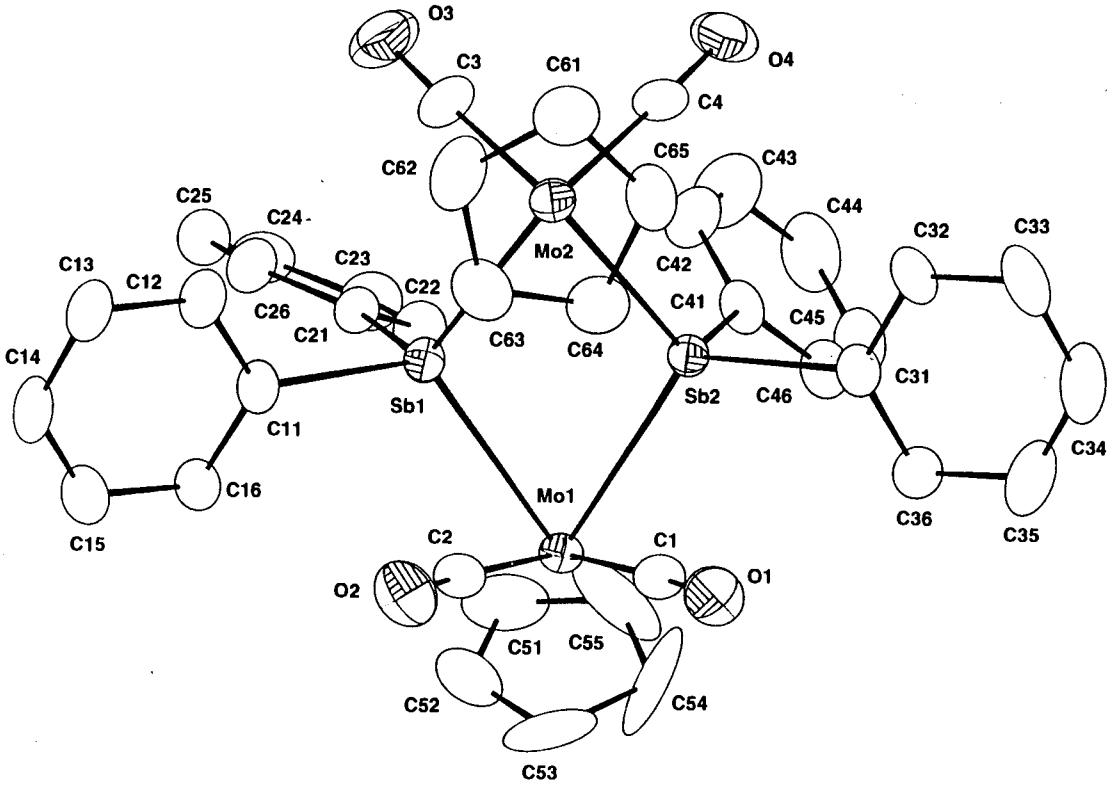

Fig. 1. Structure of $[\mu\text{-}SbPh_2]_2[Mo(CO)_2(\eta^5\text{-}C_5H_5)]_2$ **1** showing the atom numbering scheme.

2. Results and discussion

2.1. $[\mu\text{-}SbPh_2]_2[Mo(CO)_2(\eta^5\text{-}C_5H_5)]_2$ (1)

The simplest possible reaction between the antimony(V) compound $[SbPh_2BrO]_2$ and 2 mol $Na[Mo(CO)_3(\eta^5\text{-}C_5H_5)]$ would be metathesis to give $\{SbPh_2O[Mo(CO)_3(\eta^5\text{-}C_5H_5)]\}_2$ and sodium bromide. Perhaps not surprisingly, this does not occur and antimony is reduced giving among others a purple compound identified as $[\mu\text{-}SbPh_2]_2[Mo(CO)_2(\eta^5\text{-}C_5H_5)]_2$ **1**. Although the compound was prepared under Schlenk conditions, it appears to be indefinitely stable in the atmosphere.

In addition to phenyl and cyclopentadienyl bands, its IR spectrum in Nujol showed strong CO absorptions at 1924, 1870, 1857 and 1846 cm^{-1}, consistent with terminal CO groups. In CH_2Cl_2 solution strong bands at 1929 and 1866 cm^{-1} with a shoulder at 1946 cm^{-1} suggest the presence of $Mo(CO)_2$ groups, with solid state effects probably accounting for the extra bands in Nujol. The CH_2Cl_2 spectrum was comparable with those of $[Mo(CO)_2(\eta^5\text{-}C_5H_5)]_2(\mu,\eta^2\text{-}Sb_2)$ (1936 and 1885 cm^{-1}, CH_2Cl_2 solution) [8] and $[Mo(CO)_2(\eta^5\text{-}C_5H_5)]_2(\mu,\eta^2\text{-}Bi_2)$ (1917 and 1866 cm^{-1}, THF solution) [14], each containing two $Mo(CO)_2(\eta^5\text{-}C_5H_5)$ fragments in common with **1**. The presence of the 1946 cm^{-1} shoulder for **1** points to greater complexity and the possibility of more than one species in solution.

The presence of two solution species is supported by differences in the proton NMR spectra of **1** in C_6D_6 and $CDCl_3$ solutions. The C_6D_6 spectrum was fully assignable with a singlet at 4.90 ppm for the cyclopentadienyl protons and multiplets at 7.23 (*m*- and *p*-) and 7.76 (*o*-) for the phenyl protons. In $CDCl_3$, on the other hand, there were two cyclopentadienyl singlets at 5.16 and 5.32 ppm in a 4:1 ratio and the distinct separation of the *o*- and *m*- and *p*-phenyl resonances in C_6D_6 solution collapsed in $CDCl_3$ to a multiplet at 7.20–7.60 ppm. Compound **1** could, however, be recovered quantitatively from $CDCl_3$ solution and the two sets of signals are possibly associated with *cis–trans* isomerism at the molybdenum centres. The solid state structure of **1** (see below) shows a basic *trans* configuration at molybdenum and this is probably the form present in C_6D_6.

A FAB mass spectrum confirmed the molecular formula with a parent ion peak at m/z 988 while loss of 2CO gave a peak at m/z 932. Monoantimony fragments, i.e. $[SbPh_2Mo_2Cp_2(CO)_3]^+$ (m/z 685) and $[SbPh_2MoCp]^+$ (m/z 438), were observed also and there was substantial intensity for the rearrangement ion, $[SbPh_2MoCp(CO)_3]^+$, at m/z 522.

The structure of **1** as a chloroform solvate was determined by X-ray crystallography and a diagram is shown in Fig. 1. Selected bond lengths and angles are given in Table 1. The compound contains a 'butterfly'-

type Sb_2Mo_2 core, with diphenylstibido fragments bridging between 15-e$^-$ $Mo(CO)_2(\eta^5\text{-}C_5H_5)$ moieties. Both Sb–Mo [2.760(1)–2.796(1) Å] and Sb–Sb [3.0996(8) Å] separations are short; the former may imply a degree of Sb–Mo multiple bonding as the $SbPh_2$ units behave as 3-e$^-$ donors. The Sb–Mo distances are comparable with those in the stibine complex, $Mo(CO)_3[Ph_2(PhS)Sb]_3$ [mean 2.746 Å] [15], in $[Mo(CO)_2(\eta^5\text{-}C_5H_5)]_2(\mu,\eta^2\text{-}Sb_2)$ [2.762 Å] [8] and $(\mu\text{-}Sb)_2Mo_5(CO)_{14}(\eta^5\text{-}C_5H_5)_4$ [2.764 Å] [16].

The Sb–Sb separation [3.0996(8) Å] is longer than those in *cyclo*-$(PhSb)_6$ (2.837 Å) [17] and $[(Me_3Si)_2Sb]_2$ (2.867 Å) [18] but is comparable with that in $(\mu\text{-}Sb)_2Mo_5(CO)_{14}(\eta^5\text{-}C_5H_5)_4$ [3.050 Å] [16]. It is difficult to know if this is a real bond or simply a consequence of constraints within the Sb_2Mo_2 ring. The Mo(1)···Mo(2) separation [4.405(1) Å], on the other hand, implies no bonding between these atoms.

Coordination about antimony is distorted tetrahedral with angles ranging between 104.46(3) [Mo(1)–Sb(1)–Mo(2)] and 117.5(3)° [Mo(2)–Sb(1)–C(21)]; bonds to the phenyl *ipso* carbons [2.141(9)–2.16(1) Å] are unexceptional. Each molybdenum atom is attached to an η^5-cyclopentadienyl group and two carbonyl ligands, giving overall 'four-legged piano-stool' geometry, with distances to the carbonyl carbons [1.94(1)–1.96(1) Å] and to the centroid of the Cp rings [2.00 Å] comparable with those in related compounds. A view down the Sb···Sb vector (see Fig. 2) shows that the Cp rings are arranged in a near *trans* configuration.

Table 1
Selected bond distances (Å) and angles (°), with estimated S.D.s in parentheses, for $[\mu\text{-}SbPh_2]_2[Mo(CO)_2(\eta^5\text{-}C_5H_5)]_2\cdot CHCl_3$ (**1**)

Sb(1)···Sb(2)	3.0996(8)	Mo(1)–Sb(1)–Mo(2)	104.46(3)
Sb(1)–Mo(1)	2.796(1)	Mo(1)–Sb(1)–C(11)	114.6(3)
Sb(1)–Mo(2)	2.777(1)	Mo(2)–Sb(1)–C(11)	113.9(3)
Sb(1)–C(11)	2.141(9)	Mo(1)–Sb(1)–C(21)	114.4(3)
Sb(1)–C(21)	2.16(1)	Mo(2)–Sb(1)–C(21)	117.5(3)
Sb(2)–Mo(1)	2.774(1)	C(11)–Sb(1)–C(21)	92.3(4)
Sb(2)–Mo(2)	2.760(1)	Mo(1)–Sb(2)–Mo(2)	105.51(3)
Sb(2)–C(31)	2.152(9)	Mo(1)–Sb(2)–C(31)	116.8(3)
Sb(2)–C(41)	2.151(9)	Mo(2)–Sb(2)–C(31)	114.5(3)
Mo(1)–C(1)	1.94(1)	Mo(1)–Sb(2)–C(41)	109.9(3)
Mo(1)–C(2)	1.94(1)	Mo(2)–Sb(2)–C(41)	115.9(3)
Mo(1)–C(51)	2.34(1)	C(31)–Sb(2)–C(41)	94.3(3)
Mo(1)–C(52)	2.29(1)	Sb(1)–Mo(1)–Sb(2)	67.63(2)
Mo(1)–C(53)	2.26(1)	Sb(1)–Mo(1)–C(1)	116.6(3)
Mo(1)–C(54)	2.27(1)	Sb(2)–Mo(1)–C(1)	76.9(3)
Mo(1)–C(55)	2.30(1)	Sb(1)–Mo(1)–C(2)	75.4(3)
Mo(1)–Cp_{cent}	2.00	Sb(2)–Mo(1)–C(2)	114.8(3)
Mo(2)–C(3)	1.96(1)	C(1)–Mo(1)–C(2)	74.4(4)
Mo(2)–C(4)	1.94(1)	Sb(1)–Mo(2)–Sb(2)	68.09(3)
Mo(2)–C(61)	2.29(1)	Sb(1)–Mo(2)–C(3)	79.2(4)
Mo(2)–C(62)	2.31(1)	Sb(2)–Mo(2)–C(3)	121.9(3)
Mo(2)–C(63)	2.36(1)	Sb(1)–Mo(2)–C(4)	122.7(4)
Mo(2)–C(64)	2.36(1)	Sb(2)–Mo(2)–C(4)	79.2(3)
Mo(2)–C(65)	2.32(1)	C(3)–Mo(2)–C(4)	80.2(5)
Mo(2)–Cp_{cent}	2.00	Mo(1)–C(1)–O(1)	176.0(9)
O(1)–C(1)	1.17(1)	Mo(1)–C(2)–O(2)	175.0(10)
O(2)–C(2)	1.15(1)	Mo(2)–C(3)–O(3)	176.6(11)
O(3)–C(3)	1.15(1)	Mo(2)–C(4)–O(4)	178.2(11)
O(4)–C(4)	1.17(1)		

The overall structure closely resembles that of $Cu_2(PMe)_4[\mu\text{-}(mesityl)_2Sb]_2$ [19], where diarylstibido groups again bridge between related 15-e$^-$ metal fragments. Antimony coordination geometry is similar in the two cases, although the M–Sb–M angle in **1** is considerably more'open' [mean 104.99°] than in the copper compound [mean 95.11°].

Although the mechanism of formation of **1** is not known, a possible route is via $SbPh_2[Mo(CO)_3(\eta^5\text{-}C_5H_5)]$ **2** followed by CO loss and dimerisation. Similar reactions, i.e. loss of CO and phosphine, respectively, from $AsMe_2[Mo(CO)_3(\eta^5\text{-}C_5H_5)]$ [20,21] and $AsMe_2[Mo(CO)_2(PR_3)(\eta^5\text{-}C_5H_5)]_2$ [22] followed by dimerisation, both give $[\mu\text{-}AsMe_2]_2[Mo(CO)_2(\eta^5\text{-}C_5H_5)]_2$.

An attempt to prepare **2** by treating $SbPh_2Cl$ with $Na[Mo(CO)_3(\eta^5\text{-}C_5H_5)]$ in THF gave an inseparable mixture but ^{1}H-NMR spectra pointed to $SbPh_2[Mo(CO)_3(\eta^5\text{-}C_5H_5)]$ **2** as the probable major component. A related reaction between $SbPh_2Cl$ and $Na[W(CO)_3(\eta^5\text{-}C_5H_5)]$ also gave an inseparable mixture, with probably $SbPh_2[W(CO)_3(\eta^5\text{-}C_5H_5)]$ **3** as the major product from ^{1}H-NMR and FAB mass spectrometry.

2.2. $SbPh[Fe(CO)_2(\eta^5\text{-}C_5H_5)]_2$ (4) and $SbPh_2[Fe(CO)_2(\eta^5\text{-}C_5H_5)]$ (5)

The reaction of $[SbPh_2BrO]_2$ with 2 mol $Na[Fe(CO)_2(\eta^5\text{-}C_5H_5)]$ did not yield the iron analogue of **1** and gave only unidentified products, but with $SbPh_2Cl$ $Na[Fe(CO)_2(\eta^5\text{-}C_5H_5)]$ gave a mixture of $SbPh[Fe(CO)_2(\eta^5\text{-}C_5H_5)]_2$ **4** and $SbPh_2[Fe(CO)_2(\eta^5\text{-}C_5H_5)]$ **5**. The compounds could not be separated by fractional crystallisation and were characterised spectroscopically as the mixture. The crystal structure of **4** was, however, determined using well formed crystals, separated manually from the mixture.

At first sight, it is surprising that a mixture of products is obtained from this reaction, when good yields of $SbMe_2Fe(CO)_2(\eta^5\text{-}C_5H_5)$ and $SbBr_2Fe(CO)_2(\eta^5\text{-}C_5H_5)$ result from related reactions between $SbMe_2Br$ or $SbBr_3$ with $Na[Fe(CO)_2(\eta^5\text{-}C_5H_5)]$ [4]. Phenyl groups on antimony are, however, known to be labile [23] and $[Ni_{10}(SbPh)_2(CO)_{18}]^{2-}$, for example, is the major product when $SbPh_2Cl$ is treated with $[Ni_6(CO)_{12}]^{2-}$ [3].

Both **4** and **5** contain only terminal CO groups (bands at 1995, 1977 and 1946 cm^{-1}) from IR spectroscopy in THF solution and there were ^{1}H-NMR signals (C_6D_6 solution) at 4.35 (s, C_5H_5), 7.27 (m, *m*- and *p*-Ph) and 8.19 (d, *o*-Ph) for **4** and at 4.12 (s, C_5H_5), 7.27 (m, *m*- and *p*-Ph) and 7.92 (d, *o*-Ph) for **5**.

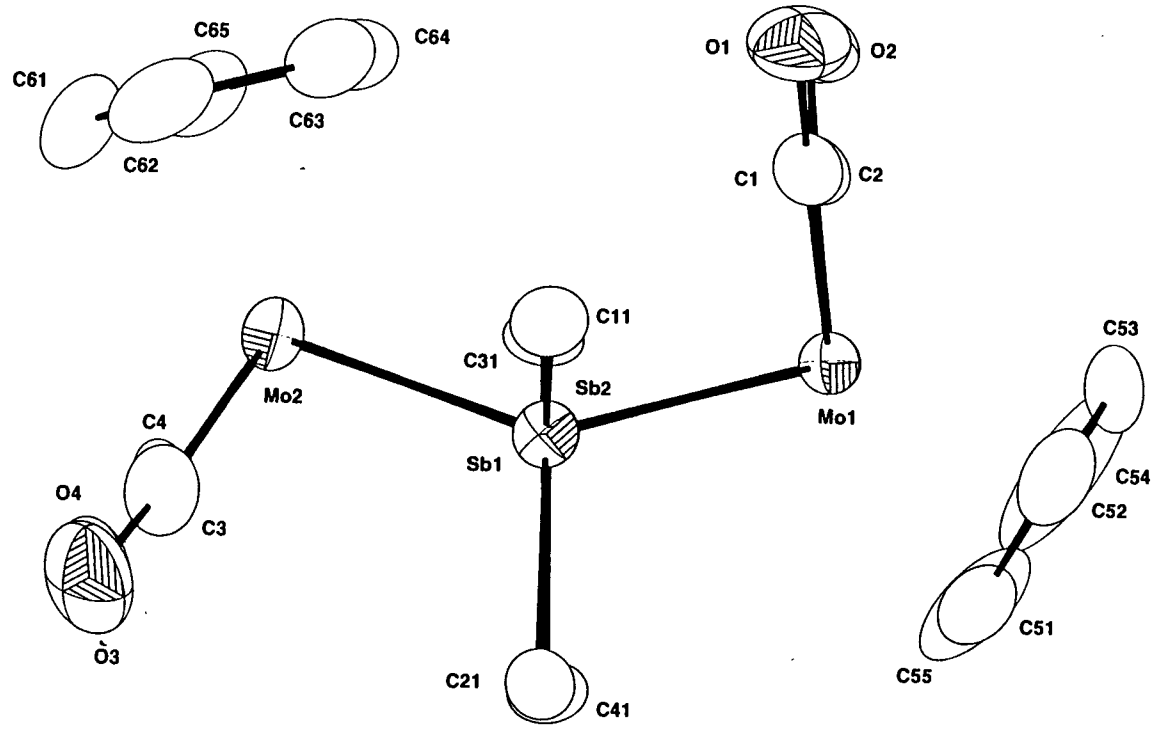

Fig. 2. Structure of $[\mu\text{-SbPh}_2]_2[\text{Mo(CO)}_2(\eta^5\text{-C}_5\text{H}_5)]_2$ **1** projected down the Sb···Sb vector.

The stoichiometry of the compounds was confirmed by EI mass spectrometry which showed parent ion peaks for both species. Low intensity peaks also indicated the successive loss of all four CO molecules from **4** and for **5**, there was a peak associated with loss of two CO molecules. The most intense peaks were assigned to fragments common to both compounds, i.e. CpFe(CO)_2^+, CpFe(CO)^+ and CpFe^+, together with SbPh^+ and SbPh_2^+, respectively, for **4** and **5**.

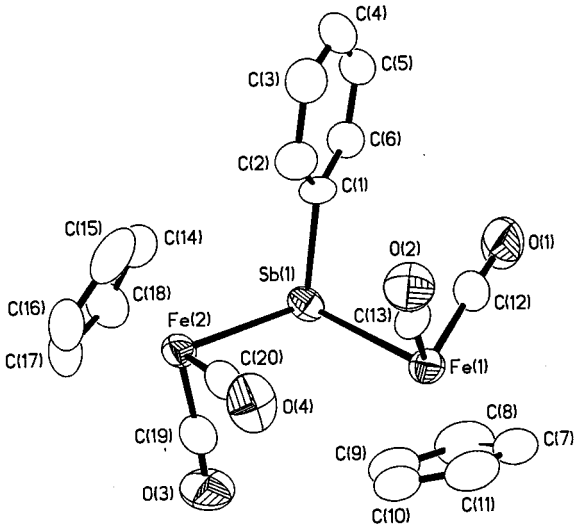

Fig. 3. Structure of $\text{SbPh[Fe(CO)}_2(\eta^5\text{-C}_5\text{H}_5)]_2$ **4** showing the atom numbering scheme.

The X-ray structure of **4**, shown in Fig. 3, consists of a phenylstibinidene fragment bridging between two 17-e$^-$ CpFe(CO)_2 units. Selected bond lengths and angles are listed in Table 2. The geometry at antimony is pyramidal with angles ranging between 98.7(2) [C(1)–Sb(1)–Fe(1)] and 111.96(5)° [Fe(1)–Sb(1)–Fe(2)] and

Table 2
Selected bond distances (Å) and angles (°), with estimated S.D.s in parentheses, for $\text{SbPh[Fe(CO)}_2(\eta^5\text{-C}_5\text{H}_5)]_2$ (**4**)

Sb(1)–Fe(1)	2.639(2)	Fe(1)–Sb(1)–Fe(2)	111.96(5)
Sb(1)–Fe(2)	2.634(1)	C(1)–Sb(1)–Fe(1)	98.7(2)
Sb(1)–C(1)	2.177(9)	C(1)–Sb(1)–Fe(2)	102.2(3)
Fe(1)–C(12)	1.74(1)	C(12)–Fe(1)–C(13)	95.1(5)
Fe(1)–C(13)	1.737(8)	C(12)–Fe(1)–Sb(1)	84.8(3)
Fe(1)–C(7)	2.10(1)	C(13)–Fe(1)–Sb(1)	89.9(3)
Fe(1)–C(8)	2.07(1)	C(19)–Fe(2)–C(20)	94.7(4)
Fe(1)–C(9)	2.12(1)	C(19)–Fe(2)–Sb(1)	86.3(3)
Fe(1)–C(10)	2.11(1)	C(20)–Fe(2)–Sb(1)	91.9(3)
Fe(1)–C(11)	2.09(1)	O(1)–C(12)–Fe(1)	176.0(11)
Fe(1)–Cp_{cent}	1.73	O(2)–C(13)–Fe(1)	174.3(8)
Fe(2)–C(19)	1.75(1)	O(3)–C(19)–Fe(2)	177.0(9)
Fe(2)–C(20)	1.75(1)	O(4)–C(20)–Fe(2)	177.0(8)
Fe(2)–C(14)	2.12(1)		
Fe(2)–C(15)	2.10(1)		
Fe(2)–C(16)	2.09(1)		
Fe(2)–C(17)	2.097(9)		
Fe(2)–C(18)	2.08(1)		
Fe(2)–Cp_{cent}	1.73		
O(1)–C(12)	1.15(1)		
O(2)–C(13)	1.140(9)		
O(3)–C(19)	1.16(1)		
O(4)–C(20)	1.14(1)		

the sum of angles [312.86°] points to a more closed arrangement than that in $Sb[Fe(CO)_2(\eta^5\text{-}C_5H_5)]_3$ [5]. Sb–Fe lengths are identical (mean 2.637 Å) and are comparable with the single bonds in $Sb[Fe(CO)_2(\eta^5\text{-}C_5H_5)]_3$ [mean 2.652 Å] [5] and $\{SbCl[Fe(CO)_2(\eta^5\text{-}C_5H_5)]_3\}_2[FeCl_4]$ [mean 2.539 Å] [24].

The overall arrangement at iron is the familiar $CpML_3$ 'three-legged piano stool', with identical Fe–C(O) [1.737(8) – 1.75(1) Å] and Fe–Cp_{cent} [1.73 Å] separations and the *trans* orientation of the cyclopentadienyl rings is similar to that in $SbCl[Mo(CO)_3(\eta^5\text{-}C_5H_5)]_2$ [5]. There is a difference in the phenyl group orientation with respect to the two Sb–Fe bonds from C(2)–C(1)–Sb(1)–Fe(1) and C(2)–C(1)–Sb(1)–Fe(2) torsion angles of −81.0(8) and 33.9(9)°, respectively.

3. Experimental

All reactions were carried out using Schlenk techniques under an argon atmosphere and the products were subsequently handled in a dry oxygen-free glovebox.

3.1. Preparation of $[\mu\text{-}SbPh_2]_2[Mo(CO)_2(\eta^5\text{-}C_5H_5)]_2 \cdot CHCl_3$ (1)

A solution of sodium cyclopentadienylide (528 mg, 4.26 mmol) in THF (40 ml) was added to molybdenum hexacarbonyl (1.142 g, 4.33 mmol) in THF (40 ml) and the resulting solution refluxed with stirring for 18 h (CARE CO evolution). After cooling, the pale yellow–green solution was added to a stirred slurry of $[SbPh_2BrO]_2$ (1.580 g, 2.12 mmol) in THF (50 ml) at −80°C. The reaction mixture, after warming to room temperature (r.t.) and stirring for a further 24 h, was filtered and evaporated to dryness in a vacuum. The remaining solid was then extracted into dichloromethane (50 ml), the solution filtered and again evaporated to dryness to give a purple solid. Pure **1** was obtained by column chromatography (CH_2Cl_2/hexane 2:5 v/v, Al_2O_3). Yield 250 mg (12% based on $[SbPh_2BrO]_2$). M.p. 259–262°C (dec.). ^{1}H-NMR (250 MHz, C_6D_6, r.t.): δ 4.90 (10H, s, *Cp*-Mo), 7.23 (12H, m, *m*- and *p*-Ph), 7.76 (8H, m, *o*-Ph). ^{1}H-NMR (250 MHz, $CDCl_3$, r.t.): δ 5.16 (10H, s, *Cp*-Mo major isomer), 5.32 (10H, s, *Cp*-Mo minor isomer), 7.32 (20H, m, *Ph*-Sb both isomers). IR (CH_2Cl_2 solution): 1946m,sh, 1929vs, 1866m,br cm^{-1}. IR (nujol mull, CsI): 1924vs, 1870m, 1857s, 1846s, 1431m, 1062w, 1019w, 819w, 736w, 728w, 696w, 556w, 549w, 449w cm^{-1}. MS (FAB, $m/z > 400$), m/z (rel. int.(%)): 988 ($Sb_2Ph_4Mo_2Cp_2(CO)_4^+$, 6), 932 ($Sb_2Ph_4Mo_2Cp_2(CO)_2^+$, 7), 876 ($Sb_2Ph_4Mo_2Cp_2^+$, 2), 685 ($SbPh_2Mo_2Cp_2(CO)_3^+$, 6), 522 ($SbPh_2MoCp(CO)_3^+$, 18), 438 ($SbPh_2MoCp^+$, 14). Found: C, 46.0; H, 3.2: $C_{38}H_{30}O_4Mo_2Sb_2$ Calc.: C, 46.3; H, 3.1%

3.2. Reaction between $SbPh_2Cl$ and $Na[Mo(CO)_3(\eta^5\text{-}C_5H_5)]$

A solution of $Na[Mo(CO)_3(\eta^5\text{-}C_5H_5)]$ prepared as above from NaCp and molybdenum hexacarbonyl (1.923 g, 7.28 mmol) in THF (35 ml) was added to a stirred solution of $SbPh_2Cl$ (2.187 g, 7.02 mmol) in THF (25 ml) at −45°C giving an immediate purple colouration. After stirring for a further 24 h at r.t., the mixture was filtered through Celite and evaporated to dryness giving an oily red product. Crystallisation from toluene gave a red powder which spectroscopy showed was a mixture of compounds that could not be separated by recrystallisation; the major component was considered to be $SbPh_2[Mo(CO)_3(\eta^5\text{-}C_5H_5)]$ **2**. ^{1}H-NMR (C_6D_6, 250 MHz, r.t.): δ 4.78 (5H, s, *Cp*-Mo), 7.21 (6H, m, *m*- and *p*-Ph), 7.80 (4H, m, *o*-Ph).

3.3. Reaction between $SbPh_2Cl$ and $Na[W(CO)_3(\eta^5\text{-}C_5H_5)]$

A solution of NaCp (847 mg, 7.23 mmol) in diglyme (40 ml) was added to tungsten hexacarbonyl (2.544 g, 7.23 mmol) in diglyme (40 ml) and the mixture stirred under reflux for 18 h. The $Na[W(CO)_3(\eta^5\text{-}C_5H_5)]$ thus formed was added to a stirred solution of $SbPh_2Cl$ (2.227 g, 7.15 mmol) in THF (20 ml) at −65°C and the mixture slowly warmed to r.t. and stirred for a further 16 h. Insolubles were filtered off through Celite and the solvent removed in a vacuum. ^{1}H-NMR spectroscopy showed that the product was a mixture that could not be separated by recrystallisation; the major component was considered to be $SbPh_2[W(CO)_3(\eta^5\text{-}C_5H_5)]$ **3**. ^{1}H-NMR (C_6D_6, 250 MHz, r.t.): δ 4.66 (s, 5H, *Cp*-W), 7.27 (6H, m, *m*- and *p*-Ph), 7.84 (4H, d, $^3J_{HH} = 7.5$ Hz, *o*-Ph). IR (CH_2Cl_2 solution): 2027m, 1995s, 1933vs,br, 1889s cm^{-1}. MS (FAB), m/z (rel. int.(%)): 608 ($SbPh_2WCp(CO)_3^+$, 2), 580 ($SbPh_2WCp(CO)_2^+$, 8), 524 ($SbPh_2WCp^+$, 11), 503 ($SbPhWCp(CO)_2^+$, 32), 447 ($SbPhWCp^+$, 37), 275 ($SbPh_2^+$, 53), 198 ($SbPh^+$, 18).

3.4. Reaction between $SbPh_2Cl$ and $Na[Fe(CO)_2(\eta^5\text{-}C_5H_5)]$

$Na[Fe(CO)_2(\eta^5\text{-}C_5H_5)]$ was prepared by adding a slurry of $[Fe(CO)_2(\eta^5\text{-}C_5H_5)]_2$ (1.393 g, 3.94 mmol) and THF (30 ml) to sodium amalgam (37 g, 0.593% w/w, 8.7 mmol Na) and the mixture stirred for 48 h. The resulting solution was filtered into a solution of $SbPh_2Cl$ (2.392 g, 7.68 mmol) in THF (50 ml) at −80°C and the mixture stirred at r.t. for 24 h. After filtration through Celite, the solution was reduced to ca. 10 ml and overlayered with hexane (30 ml) to give, after 3 days at −30°C, crystals shown spectroscopically to be a mixture of $SbPh[Fe(CO)_2(\eta^5\text{-}C_5H_5)]_2$ **4** and $SbPh_2[Fe(CO)_2(\eta^5\text{-}C_5H_5)]$ **5**. Attempts to separate the

compounds by recrystallisation were unsuccessful and they were characterised as the mixture. Yield 2.03 g. IR (THF solution, mixture): 1995vs, 1977m, 1946vs cm^{-1}.

$SbPh[Fe(CO)_2(\eta^5\text{-}C_5H_5)]_2$ **4**: ^{1}H-NMR (250 MHz, C_6D_6, r.t.): δ 4.35 (10H, s, *Cp*-Fe), 7.27 (3H, m, *m*- and *p*-Ph), 8.19 (2H, d, $^3J_{HH} = 6.5$ Hz, *o*-Ph). MS (EI), *m*/*z* (rel. int.(%)): 552 ($SbPhFe_2Cp_2(CO)_4^+$, 3), 524 ($SbPhFe_2Cp_2(CO)_3^+$, 0.5), 496 ($SbPhFe_2Cp_2(CO)_2^+$, 1), 468 ($SbPhFe_2Cp_2(CO)^+$, 1), 440 ($SbPhFe_2Cp_2^+$, 3), 198 ($SbPh^+$, 22), 177 ($FeCp(CO)_2^+$, 22), 149 ($FeCp(CO)^+$, 21), 121 ($FeCp^+$, 100), 77 (Ph^+, 9), 56 ($C_2O_2^+$, 41).

$SbPh_2[Fe(CO)_2(\eta^5\text{-}C_5H_5)]$ **5**: ^{1}H-NMR (250 MHz, C_6D_6, r.t.): δ 4.12 (5H, s, *Cp*-Fe), 7.27 (6H, m, *m*- and *p*-Ph), 7.92 (4H, d, $^3J_{HH} = 6.2$ Hz, *o*-Ph). MS (EI), *m*/*z* (rel. int.(%)): 452 ($SbPh_2FeCp(CO)_2^+$, 3), 396 ($SbPh_2FeCp^+$, 18), 275 ($SbPh_2^+$, 11) and Fe/Cp/CO as for **4**.

3.5. Crystal structure determinations for $[\mu\text{-}SbPh_2]_2[Mo(CO)_2(\eta^5\text{-}C_5H_5)]_2.CHCl_3$ (1) and $SbPh[Fe(CO)_2(\eta^5\text{-}C_5H_5)]_2$ (4)

Crystals of **1** suitable for X-ray crystallography were obtained by slow diffusion of hexane into a concentrated chloroform solution and crystals of **4** were hand picked from the mixture. Crystal data and details of the structure solutions are summarised in Table 3. For **1**, data were collected on a Hilger and Watts Y290 diffractometer and corrected for Lorentz and polarisation effects and for absorption (DIFABS) [25]. The structure was solved by Patterson and Fourier difference syntheses and refined using the CRYSTALS programs [26]. Hydrogen atoms were placed at calculated positions [*d*(C–H) 1.0 Å] and refined with fixed isotropic thermal parameters, riding on the attached carbon atom. The chloroform molecule was disordered.

For **4**, slightly more than one hemisphere of data was collected on a Delft Instruments FAST TV area detector diffractometer, equipped with a rotating anode FR591 generator [27]. The data were corrected for Lorentz and polarisation effects and for absorption (Ψ-scans). The structure was solved by direct methods (SHELXS-86) [28] and Fourier difference syntheses and refined on F_o^2 by full-matrix least-squares using all unique data (SHELXL-93) [29]. Hydrogen atoms were placed at calculated positions [*d*(C–H) 0.95 Å] and refined with fixed isotropic thermal parameters, riding on the attached carbon atom.

Table 3
Crystallographic data for compounds **1** and **4**

Compound	**1**	**4**
Chemical formula	$C_{39}H_{31}Cl_3Mo_2O_4Sb_2$	$C_{20}H_{15}Fe_2O_4Sb$
Formula weight	1105.4	552.8
Crystal size (mm)	$0.45\times0.25\times0.20$	$0.50\times0.40\times0.20$
Crystal system	Monoclinic	Orthorhombic
Space group	$P2_1/c$	$Pca2_1$
a (Å)	14.662(3)	18.003(4)
b (Å)	14.896(3)	7.634(2)
c (Å)	18.759(4)	14.521(3)
β (°)	107.54(1)	90
Volume (Å^3)	3906.5	1995.7
Z	4	4
$D_{calc.}$ (g cm^{-3})	1.880	1.840
Radiation (Å)	Mo–K_α (0.71069)	Mo–K_α (0.71069)
μ (cm^{-1})	22.36	28.00
F(000)	2136	1080
θ limits (°)	2–25	2–30
Index ranges (for unique data)	$-15<h<14$, $0<k<15$, $0<l<19$	$-1<h<25$, $0<k<10$, $0<l<20$
Temperature (K)	298	298
Total data collected	5059	3215
Unique data	5059	3001
R_{int}		0.0593
Absorption correction	DIFABS	Numerical
Min	0.885	0.406
Max	1.116	0.956
Structure solution	Patterson (SHELXS-86)	Direct methods (SHELXS-86)
Refinement	Full-matrix least-squares on *F*	Full-matrix least-squares on F^2
Data/variables	4028/432	2945/245
Goodness-of-fit (*S*)	1.038	0.848
Final diff. map (e Å^{-3})	+2.08, −1.50	+0.80, −1.666
R observed data [$I>2\sigma(I)$]	0.0488	0.0340
R_w all data	0.0542	0.258

4. Supplementary material available

Full details of the atomic parameters and bond lengths and angles have been deposited with the Cambridge Crystallographic Data Centre.

Acknowledgements

We thank Professor M.B. Hursthouse and the EPSRC Crystallographic Service for X-ray data collection on **4**.

References

[1] R.F. Bryan, W.C. Schmidt Jr., J. Chem. Soc. Dalton Trans. (1974) 2337.
[2] J. von Seyerl, G Huttner, Cryst. Struct. Comm. 9 (1980) 1099.
[3] R.E. DesEnfants II, J.A. Gavney Jr., R.K. Hayashi, A.D. Rae, L.F. Dahl, A. Bjarnason, J. Organomet. Chem. 383 (1990) 543.
[4] P. Panster, W. Malisch, Chem. Ber. 109 (1976) 692.
[5] A.M. Barr, M.D. Kerlogue, N.C. Norman, P.W. Webster, L. Farrugia, Polyhedron 8 (1989) 2495.
[6] W. Malisch, P. Panster, Chem. Ber. 108 (1975) 700.
[7] N.A. Compton, R.J. Errington, G.A. Fisher, et al., J. Chem. Soc. Dalton Trans. (1991) 669.
[8] J.R. Harper, A.L. Rheingold, J. Organomet. Chem. 390 (1990) C36.

[9] U. Weber, G. Huttner, O. Steidsteger, L. Zsolnai, J. Organomet. Chem. 289 (1985) 357.
[10] K.H. Whitmire, in: N.C. Norman (Ed.), Chemistry of Arsenic, Antimony and Bismuth, Blackie, Glasgow, 1998, Ch. 7.
[11] W. Malisch, H.-A. Kaul, E. Gross, U. Thewalt, Angew. Chem. Int. Ed. Engl. 21 (1982) 549.
[12] Y. Yamamoto, M. Okazaki, Y. Makisaka, K.-Y. Akiba, Organometallics 14 (1995) 3364.
[13] W. Clegg, N.A. Compton, R.J. Errington, D.C.R. Hockless, N.C. Norman, M. Ramshaw, P.M. Webster, J. Chem. Soc. Dalton Trans. (1990) 2375.
[14] W. Clegg, N.A. Compton, R.J. Errington, N.C. Norman, Polyhedron 7 (1988) 2239.
[15] M. Wieber, H. Hohl, C. Buschka, Z. Anorg. Allg. Chem. 583 (1990) 113.
[16] M. Gorzellik, B. Nuber, M.L. Ziegler, J. Organomet. Chem. 431 (1992) 171.
[17] H.J. Breunig, K. Häberle, M. Dräger, T. Severengiz, Angew. Chem. Int. Ed. Engl. 24 (1985) 72.
[18] G. Becker, H. Freudenblum, C Wittauer, Z. Anorg. Allg. Chem. 492 (1982) 37.
[19] A.H. Cowley, R.A. Jones, C.M. Nunn, D.L. Westmoreland, Angew. Chem. Int. Ed. Engl. 28 (1989) 1018.
[20] P. Panster, W. Malisch, Chem. Ber. 109 (1976) 3842.
[21] W. Malisch, M. Kuhn, W. Albert, H. Rossner, Chem. Ber. 113 (1980) 3318.
[22] W. Malisch, H. Rossner, K. Keller, R. Janta, J. Organomet. Chem. 133 (1977) C21.
[23] M. Nunn, D.B. Sowerby, D.M. Wesolek, J. Organomet. Chem. 251 (1983) C45.
[24] Trinh-toan, L.F. Dahl, J. Am. Chem. Soc. 93 (1971) 2654.
[25] N.P.C. Walker, D. Stuart, Acta Crystallogr. A 39 (1983) 158.
[26] D.J. Watkin, J.R. Carruthers, D.W. Betteridge, CRYSTALS User's Guide, Chemical Crystallography Laboratory, University of Oxford, England, 1985.
[27] J.A. Darr, S.R. Drake, M.B. Hursthouse, K.M.A. Malik, Inorg. Chem. 32 (1993) 5704.
[28] G.M. Sheldrick, Acta Crystallogr. A 46 (1990) 467.
[29] G.M. Sheldrick, SHELXL93 Program for Crystal Structure Refinement, University of Göttingen, Germany, 1993.